Vol. 2, No. 5 May 1992

GSA TODAY

A Publication of the Geological Society of America

INSIDE

180 Million Years of Subduction

David C. Engebretson, Kevin P. Kelley, Harold J. Cashman
Department of Geology, Western Washington University, Bellingham, WA 98225

Mark A. Richards
Department of Geology and Geophysics, University of California, Berkeley, CA 94720

ABSTRACT

A compilation of lithosphere consumed globally in the past 180 m.y. reveals that the equivalent of the surface area of Earth has descended into the mantle, producing "lithospheric graveyards." Not evenly distributed, this subducted lithosphere lies concentrated in areas of cold mantle that correspond to gross mantle heterogeneities delineated by seismic tomography and the geoid and inversely related to the global distribution of hotspots. Some convergent margins (e.g., North American continent) show subducted lithosphere distributed over a large region beneath the land mass while others (e.g., eastern Eurasia) show an accumulation of up to 18 subducted lithospheric thicknesses in a narrow region. Differences in graveyard distribution result from displacements of trenches (assumed nearly fixed to the overriding plates) over the mantle: North America, South America, Africa, and southeastern Eurasia each advanced toward and perpendicular to their trenches by approximately 4000, 3000, 2700, and 1000 km, respectively between 150 Ma and the present. In contrast, eastern Eurasia (near Japan) first retreated by approximately 1200 km until 80 Ma and then advanced an equivalent distance to the present.

Net convergence at selected subduction zones also shows variability: in the past 150 m.y., approximately 13 000 km of lithosphere descended into the Japan and western North American trenches, approximately 8000 km under the central Andes and Himalayan regions, and about 1000 km of convergence was accommodated by the western Alps. Such extreme differences in kinematic histories may help explain contrasting orogenic styles. It appears that a large amount of convergence is not a necessary condition for orogeny (western Alps) nor is it sufficient (eastern Eurasia), whereas significant trench advance may be both necessary and sufficient, especially when the plate interaction involves at least one continent.

Previous workers have shown that a decrease in global spreading rates (based on estimating the geometry and spreading history of ridges for the past 80 m.y.) is the primary cause of a volume decrease in mid-ocean ridges and is consistent with a corresponding lowering of eustatic sea level during this time interval. We present an extension of this hypothesis to the past 180 m.y. by using our rates of global lithospheric consumption to estimate total global spreading and calculate the inferred changes in mid-ocean ridge volumes. Changes in global spreading rates do not affect the age distribution within the oceans instantaneously, because it takes a finite amount of time for significant amounts of oceanic crust to be replaced: an approximate 30 m.y. lag time is noted between first-order changes in global spreading rates and eustatic sea level. A simple model that predicts eustatic sea level using global spreading rates is in good agreement with the observed sea-level curve, especially after 120 Ma. A noted misfit in predicted and observed eustatic sea level prior to 120 Ma may indicate a long period of slow global spreading before 120 Ma. This may reflect rising mantle temperatures, consistent with a recently proposed dynamic-convection model.

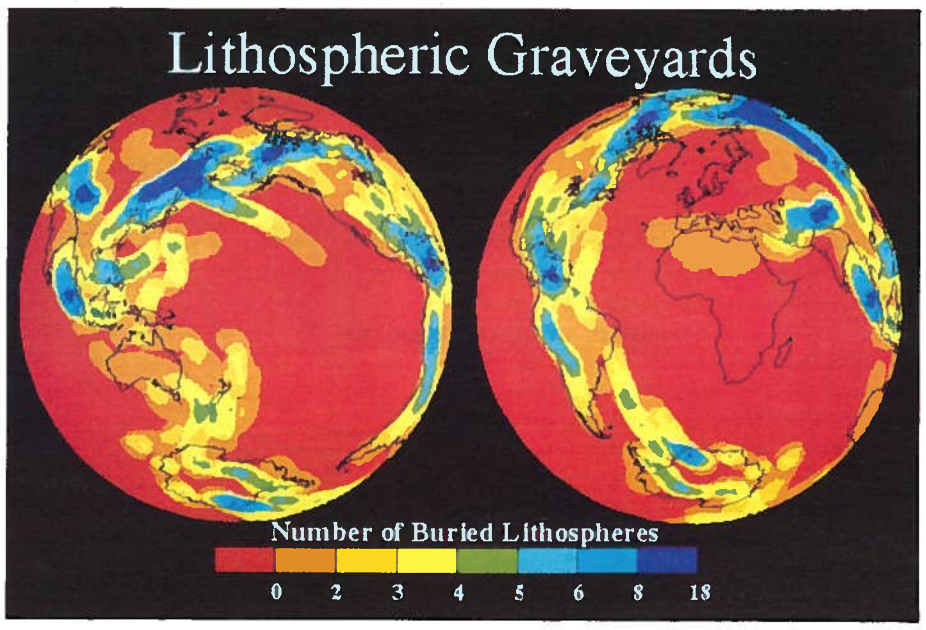

Figure 1. Locations of lithosphere subducted globally for the past 180 m.y. Dark blue areas represent the location of greater than 8, and as much as 18, km^2 of subducted lithosphere per km^2 of Earth surface area. A convenient way to interpret these values would be that *n* oceanic lithospheres were subducted below the colored areas. Red areas are locations where no plate has been subducted within this time interval. (a) Equal-area polar projection centered at lat 0°N and long 180°E; (b) Equal-area polar projection centered at lat 0°N and long 0°E.

TABLE 1. SOURCES FOR THE RECONSTRUCTION

Plate pair*	Time (Ma) From	To	Reference
PA-HS	142	0	Henderson et al. (1984)
AF-HS	180	0	Morgan (1983)
AF-NA	3	0	DeMets et al. (1990)
AF-NA	180	3	Klitgord and Schouten (1986)
EU-NA	3	0	DeMets et al. (1990)
EU-NA	105	3	Srivastava and Tapscott (1986)
AF-SA	3	0	DeMets et al. (1990)
AF-SA	133	3	Cande et al. (1988)
PA-FA	21	0	Wilson (1988)
PA-FA	180	21	Engebretson et al. (1984)
PA-KU	85	43	Engebretson et al. (1984)
PA-IZ	180	85	Engebretson et al. (1984)
PA-PH	180	115	Engebretson et al. (1984)
AN-AF	3	0	DeMets et al. (1990)
AN-AF	142	3	Molnar et al. (1988)
AU-AN	3	0	DeMets et al. (1990)
AU-AN	95	3	Stock and Molnar (1988)
IN-AF	3	0	Stock and Molnar (1988)
IN-AF	142	3	Molnar et al. (1988)
AU-NI	95	0	Weissel and Hayes (1977)
PA-NZ	3	0	DeMets et al. (1990)
PA-NZ	84	3	Pardo-Casas and Molnar (1987)
PA-NZ	180	84	Engebretson et al. (1984)

* PA: Pacific; HS: Hotspots; AF: Africa; NA: North America; EU: Eurasia; KU: Kula; IZ: Izanagi; PH: Phoenix; AN: Antarctica; AU: Australia; IN: India; NI: North Island, New Zealand; NZ: Nazca.

INTRODUCTION

Continued refinement of relative plate motions within the fixed-hotspot reference frame allows global subduction parameters to be estimated. Of prime interest is the area of lithosphere subducted annually (presented in km^2/yr) and the locations of this subducted lithosphere (referred to as lithospheric graveyards; Fig. 1). As proposed by Chase (1979), Chase and Sprowl (1983), and Richards et al. (1988), large regions containing previously subducted lithosphere should correlate with large-scale mantle heterogeneities. The relation between locations of subducted lithosphere and mantle heterogeneity was tested by Richards and Engebretson (1992) and is reviewed here.

Also of interest is the kinematic character of subduction zones in both the hotspot reference frame and in total convergence at plate boundaries. The distribution of lithospheric graveyards is a direct result of the prebreakup configuration of the subduction zones encircling Pangea, the subsequent migration of these convergent boundaries, and the net convergence at these boundaries. We selected five convergence zones and calculated the displacements over the hotspots of the overriding plates perpendicular to their boundaries and linear consumption of lithosphere descending into the mantle.

Given no net Earth expansion or contraction, calculation for the global accretion rate at oceanic ridges provides the opportunity to estimate the capacity of the world's ocean basins to hold sea water. Previous attempts were based on knowing the lengths and spreading histories of ridge systems (e.g., Pitman, 1978; Kominz, 1987) and covered the time period since 80 Ma. Our work is dependent upon knowing the geometry and plate interaction history at subduction zones, and we extend the analysis back to 180 Ma. Both methods share severe uncertainties that increase greatly as the time of interest is expanded. The methods presented here are preferred since the history of subduction is probably more completely recorded in the geologic record than past geometries of largely missing oceanic crust.

GLOBAL SUBDUCTION PARAMETERS

Finite rotations describing relative motions in the various ocean basins and between plates and hotspots given in Table 1, along with their sources, have been calibrated to the time scale of Kent and Gradstein (1986). It is beyond the scope of this paper to critically evaluate all sources of uncertainties in the model. Uncertainties grow with increasing reconstruction time such that results prior to about 150 Ma are highly speculative. Sources for errors include the fixity of hotspots (motions between Pacific and African hotspots), plate-to-hotspot motions (especially

Subduction *continued on p. 94*

Each month, *GSA Today* features a short science article on fast-breaking items or current topics of general interest to the 17,000 members of GSA. What do you think of these articles? Do you have an idea for an article that you would like to see published in *GSA Today*? If so, please contact Eldridge Moores, Science Editor, *GSA Today*, (916) 752-0352, fax 916-752-0951.

IN THIS ISSUE

GSA TODAY

May 1992
Vol. 2, No. 5

GSA TODAY (ISSN 1052-5173) is published monthly by The Geological Society of America, Inc., with offices at 3300 Penrose Place, Boulder, Colorado. Mailing address: P.O. Box 9140, Boulder, CO 80301-9140, U.S.A. Second-class postage paid at Boulder, Colorado, and at additional mailing offices. **Postmaster:** Send address changes to *GSA Today*, Membership Services, P.O. Box 9140, Boulder, CO 80301-9140.

SUBSCRIPTIONS for 1992 calendar year: **Society Members:** *GSA Today* is provided as part of membership dues. Contact Membership Services at (800) 472-1988 or (303) 447-2020 for membership information. **Nonmembers & Institutions:** $36 for U.S., Canada, and Mexico; $46 elsewhere. Contact Subscription Services (same phones). **Single copies** may be requested from Publication Sales. **Claims:** For nonreceipt or for damaged copies, members contact Membership Services; all others contact Subscription Services. Claims are honored for one year; please allow sufficient delivery time for overseas copies.

Subduction *continued from p. 93*

prior to 120 Ma), plate-to-plate displacements, plate geometries (with the possibility of missing entire plates, most notably during the early history of the Tethys), and the magnetic time scale. We experimented with end-member reconstructions and found a qualitative estimate for uncertainty in time-integrated motions to be about 20% at 100 Ma and 40% at 180 Ma.

To obtain amounts of subducted lithosphere, subduction zones were assigned to an overriding plate, digitized at their present locations and reconstructed to their former positions in a fixed-hotspot reference frame at 30 m.y. intervals. It was assumed that these convergence zones remained fixed relative to their overriding plates: we acknowledge that back-arc spreading and trench-polarity reversals introduce additional errors into the results. Critical decisions made about the location of the interacting plates were based primarily on the locations of plate boundaries within the oceans and to a lesser extent on known geologic histories. Stage poles of 5 m.y. duration that correspond to the relative motions along the length of convergence were used to calculate the area of subducted lithosphere. This area of lithosphere was then injected into the mantle at 700 km depth at a position inboard of the subduction zone, assuming a 45° dip in the downgoing plate. A reasonable physical interpretation of this method would be that lithosphere descends into the mantle at the 45° angle until it reaches 700 km; it then descends vertically into the lower mantle. The process was repeated for each of the 30 m.y. intervals back to 180 Ma and compiled globally by summing the total area of plate residing within 10° circles centered at each 1° latitude and longitude intersection. These total amounts (lying within each of the 10° circles) were divided by the area of the circle to normalize the values to Earth surface area. Figure 1 shows total area of subducted lithosphere (per Earth area) at latitude and longitude intersections and can be interpreted to represent the number of lithospheres buried beneath each location.

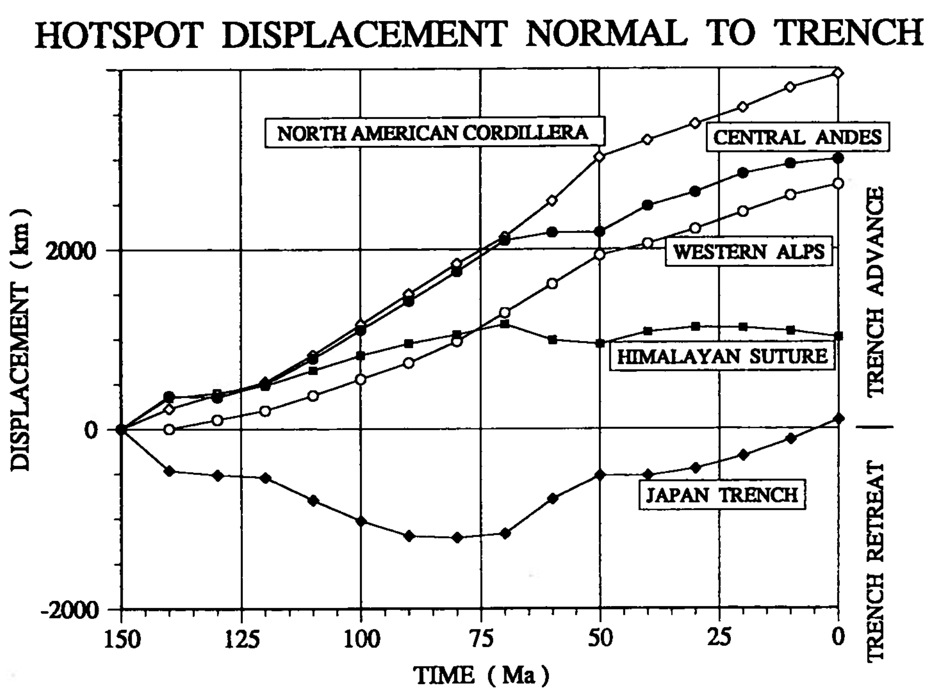

Figure 2. Components of total motion perpendicular to plate boundaries for overriding plates in the hotspot reference frame. Positive values (and slopes) represent advance of plate toward subduction zones; negative values (and slopes) show retreat. Analysis begins at 150 Ma because of the large uncertainties prior to this time. Site latitude, longitude, and trench azimuth are as follows: North American Cordillera—37°N, 236°E, 320°; central Andes—30°S, 289°E, 10°; Himalayan suture—33°N, 83°E, 270°; Japan Trench—35°N, 140°E, 205°; Western Alps—44°N, 10°E, 270°).

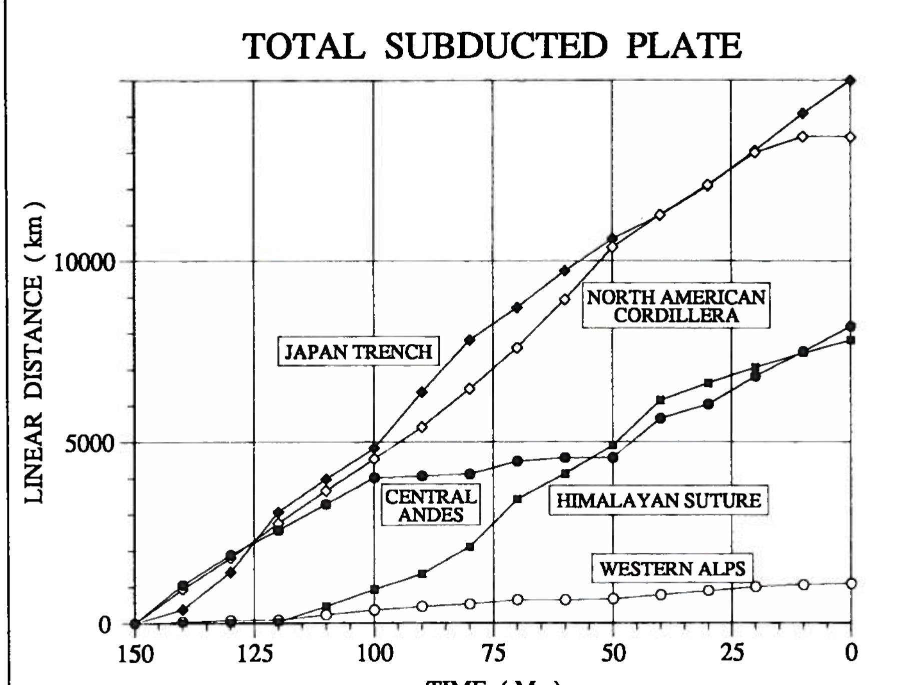

Figure 3. Total convergence perpendicular to trenches at selected sites. Amounts were calculated in a reference frame fixed to the overriding plate. Sites and azimuths are same as in Figure 2. Histories of plate interaction are as follows. North American Cordillera—Farallon 150–84 Ma, Kula 84–68 Ma, Farallon 68–10 Ma, Pacific 10–0 Ma; central Andes—Farallon 150–84 Ma, Nazca 84–0 Ma; Himalayan suture—India 150–0 Ma; Japan Trench—Izanagi 150–84 Ma, Pacific 84–0 Ma; Western Alps—Eurasia 150–0 Ma.

DISTRIBUTION OF LITHOSPHERIC GRAVEYARDS

Differences in graveyard size are the result of the 180 Ma location and subsequent migration of the overriding plate relative to the mantle (hotspots) and the total plate consumed at trenches. To investigate these relations, two kinematic compilations were made at five selected sites: the total component of displacement over the mantle normal to plate boundaries (Fig. 2), and the total amount of plate consumed (Fig. 3). For these analyses, we have restricted the treatment to post-150 Ma because of poorly determined reconstructions for the earlier record. Positive values in Figure 2 represent time-integrated motions of overriding plates advancing in the direction of their boundaries; negative values show retreat. Likewise, positive and negative slopes along the curves in Figure 2 represent rates of advance and retreat, respectively. To arrive at Figure 3, perpendicular components of subduction relative to the overriding plates (North America, South America, Eurasia, and Africa) were calculated by using the plate boundary azimuths given in the caption for Figure 2. Plate interaction histories are summarized in the caption for Figure 3.

Figures 1, 2, and 3 show the following patterns: both North America and South America advanced large distances toward their trenches (Fig. 2), thereby distributing subducted lithosphere beneath their land masses (Fig. 1), North America more so than South America. In contrast, Eurasia first retreated from the Japan Trench (between about 150 and 90 Ma) and then advanced to create the largest graveyard seen globally, a ratio of subducted plate area to Earth surface area of 18 (within the dark blue area near Japan). North America and Eurasia (near Japan) each consumed approximately 13 000 linear km of plate (Fig. 3). Near the Himalayan suture, Eurasia advanced trenchward approximately 1000 km between 150 and 75 Ma and then remained stationary (Fig. 2). In total plate consumed, Eurasia (near the Himalayan suture) and South America are similar (about 8000 km) but differ in their times of major convergence (see the pre—50 Ma curves in Fig. 3). Quite different is the kinematic history of Africa (near the western Alps) where approximately 2200 km of northward trench advance is seen since 150 Ma. Eurasia also moved northward but at a slower rate, resulting in a minimum of convergence for the sites studied (about 1000 km).

MANTLE HETEROGENEITY

Mantle heterogeneities (seen through lower mantle seismic velocities, the geoid, and global hotspot distribution; Fig. 4) have been attributed to long-term (100–200 Ma) global subduction (e.g., Chase, 1979; Chase and Sprowl, 1983; Davies, 1984; Richards et al., 1988; Anderson, 1989; Richards and Engebretson, 1992). Chase (1979) noted a qualitative correlation between a circum-Pacific band of geoid lows and post–125 Ma subduction. Davies (1984) suggested that large-scale mantle structure could lag behind rapidly changing plate boundary configurations and showed with simple convection models that the geoid could plausibly represent a thermal structure developed in the Mesozoic or earlier. Similar thermal effects from subduction encircling Pangea were discussed by Anderson (1989). Richards et al. (1988) showed that the effect of cold subducted slabs from the Cenozoic and Mesozoic was, in principle, sufficient to explain the lower mantle degree-2 seismic velocity structure as well as the geoid. Thus, they hypothesized that the amount and location of lithosphere subducted over the past 100–200 m.y. might explain the observed large-scale structure of convection. This assumes, implicitly, that mid-ocean ridges are passive structures and that mantle heterogeneity is primarily the result of subduction. This hypothesis was supported by Richards and Engebretson (1992), using the relative motion model outlined here.

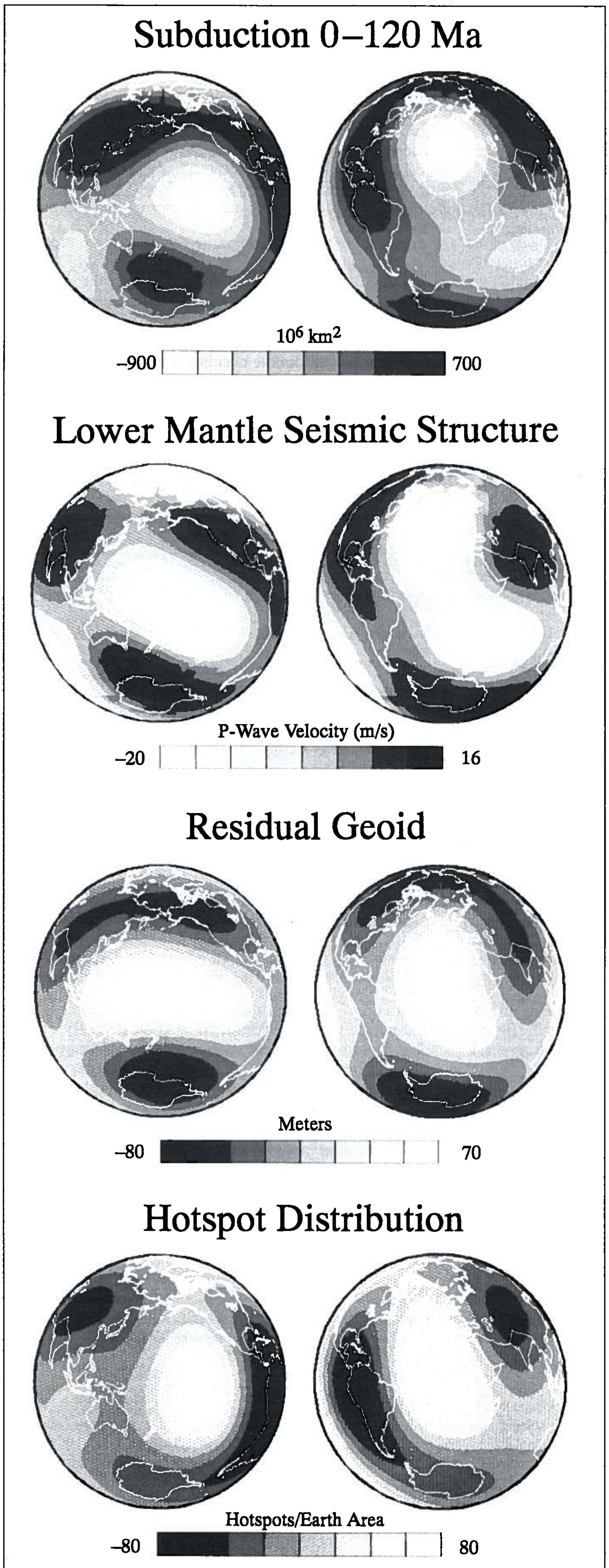

Figure 4. Comparison (from top to bottom) of spherical harmonic components (L = 2,3) of: time-integrated flux of subducted slabs since 120 Ma calculated in the hotspot fixed reference frame (Richards and Engebretson, 1992); lower mantle seismic velocity model of Dziewonski (1984); observed geoid of Lerch et al. (1983) corrected for hydrostatic figure (Nakiboglu, 1982) and upper-mantle slab signal (Hager, 1984); and hotspot distribution (Richards et al., 1988). Projections same as in Figure 1.

Figure 4 (from top to bottom) shows the general agreement found between the largest wavelengths (10 000–20 000 km) of the time-integrated flux of subducted slabs since 120 Ma, lower mantle seismic structure, residual geoid, and global hotspot distribution. The main conclusion of Richards and Engebretson (1992) was that there is a dynamically reasonable relation between plate tectonics and large-scale mantle convection—the deep mantle is cold where there has been subduction. Implicit in this work is the assumption that horizontal motions in the deep mantle are much slower than in the upper mantle. This is justified by the fact that hotspots, which presumably result from deep mantle plumes, exhibit relative motions that are much slower than relative plate motions. Therefore, we feel justified in ignoring horizontal motions of subducted slabs after they enter the lower mantle, although they probably continue to descend (nearly vertically).

ACCRETION RATES AND SEA LEVEL

During periods of rapid seafloor spreading, young (hot) ocean floor displaces older (cold) parts of the seafloor, causing the volume of the world's ocean basins to decrease (Pitman, 1978). Gurnis (1990) has questioned this relation by pointing out that the effect of increased spreading rates is to increase the amount of cold lithosphere injected into the mantle, significantly changing the deep thermal structure under oceans and continents. Increased injection of cold lithosphere reduces the volume of sublithospheric mantle, causing the volume of the ocean basins to increase, most notably when subduction occurs within the ocean basins.

The primary difference between the dynamic-convection model (Gurnis, 1990) and the lithosphere-subsidence model (Pitman, 1978) occurs about 100 m.y. after a significant change in spreading from steady spreading rates (Fig. 2 in Gurnis, 1990). Hager (1980) presented a dynamical model in which sea level could either rise or fall with increased spreading. If lithospheric slabs are primarily injected into mantle beneath the oceans, the overriding plate is pulled down, which increases the volume of the oceans and lowers sea level; if slabs are primarily subducted beneath continents, the local effect is to pull down the continent and locally produce a sea-level rise. Sea level will rise or fall according to increased or decreased spreading only when subcontinental and suboceanic mantles are cooled equally by subducted lithosphere (Hager, 1980). We will return to these discussions after presenting our attempt to model sea level using only the lithospheric-subsidence model.

Previous estimates for the effect of variations in global spreading rates (e.g., Pitman, 1978; Kominz, 1987) have focused on knowing the lengths and spreading rates of all the world's ridge systems. In contrast, the method used here infers spreading rates from global subduction rates. Global spreading rates were derived by summing the total area of subducted lithosphere through 5 m.y. time intervals (Fig. 5). Interestingly, the grand total of subducted lithosphere (area under curve in Fig. 5) is approximately 525×10^6 km^2, nearly equal to the surface area of Earth. Included in Figure 5 is eustatic sea level (Haq et al., 1987) averaged through a 10 m.y. running window. Note the approximate 30 m.y. lag time between greatest accretion rate and highest sea level (dashed line in Fig. 5).

Pitman (1978) and Kominz (1987) have demonstrated the importance that spreading rates have in regard to changes in sea level by estimating the lengths and spreading rates of ridges, calculating ridge bathymetry from the age-depth relation (Sclater et al., 1971; Parsons and Sclater, 1977), and interpreting corresponding volume changes assuming they knew the shape and size of the ocean basins being filled or drained. General agreement between their work and estimates of eustatic sea level from seismic stratigraphy (e.g., Vail et al., 1977; Haq et al., 1987) support a causal relation. Kominz (1987) presented the most complete analysis of these relations to date, analyzed sources of error, produced several reconstruction stages estimating ridge volumes, and showed that the primary cause of a decrease in ridge volume since the Late Cretaceous was a decrease in spreading rates. Kominz (1987) noted that ridges within the Pacific basin dominate the results; several important discrepancies in ridge geometries exist between Kominz's (1987) work and our own (Engebretson et al., 1984, 1985). Whereas the work of Kominz (1987) was an excellent attempt at a difficult problem, some improvements are possible given that there are new reconstructions available for nearly all plate pairs and improved reconstructions for the hotspot reference frame. Moreover, by reconstruction of the subduction history we were able to extend the analysis back to 180 Ma. Results back to 120 Ma are reasonably successful; poor agreement (Fig. 6) is seen between 180 and 120 Ma, presumably due either to our inability to decipher earlier plate displacements or to processes involved in the dynamic-convection model.

Subduction *continued on p. 100*

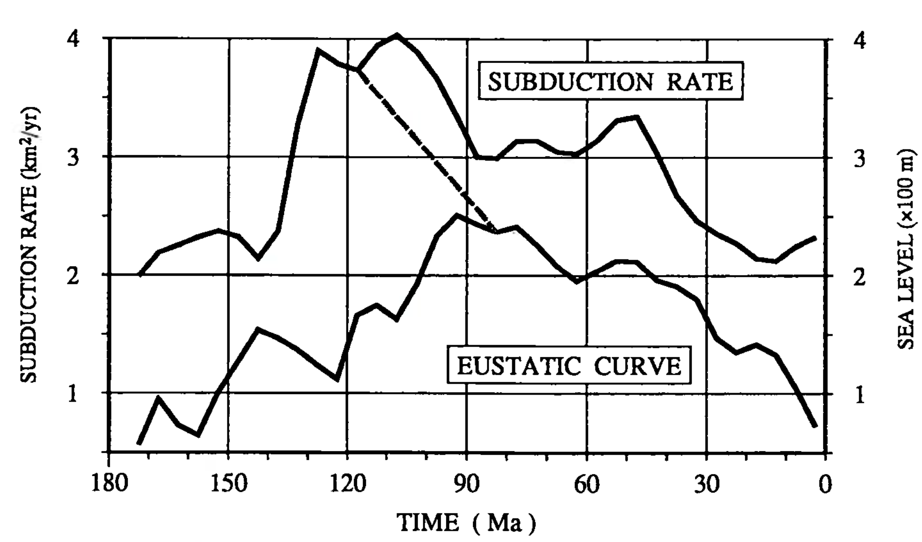

Figure 5. Subduction rate vs. time (upper curve) and the eustatic sea-level curve of Haq et al. (1987). Both curves have been smoothed with a 10 m.y. running window. Dashed curve shows approximate 30 m.y. lag time between maximum spreading rates and highest sea level.

Subduction *continued from p. 95*

We analyzed the effect that changes in global spreading rates have on eustatic sea level (lithosphere subsidence model) by modeling the age-area distribution within the oceans at 1 m.y. increments. Predicted changes in sea level were based on the following methods and assumptions.

1. Assume a linear decrease in the age-area distribution for a 180 Ma ocean basin as observed in today's oceans (Parsons, 1982). As noted below, various beginning models can be used. One simply "builds" an ocean basin with a chosen spreading rate and assigns the age distribution according to the relation (from Parsons, 1982): area (age) = rate (1 – age/180), where area = 10^6 km^2 of a given age, age = m.y., and rate = areal spreading rate (10^6 km^2/m.y.).

2. Assume that no plate older than 180 Ma is preserved. Thus, at each 1 m.y. interval, remove all of the plate that is older than 180 Ma.

3. The percentage of plate of a given age (younger than 180 Ma) removed from the model depends upon the percentage of plate that age present. Assume that the total amount subducted equals the amount formed.

4. Calculate the volume of the ocean basin at each step by using the age-depth relation of Parsons and Sclater (1977).

5. Calculate the resulting change in sea level from the relation, provided by Pitman (1978), that assumes a known shape and size of the ocean basin being filled or drained.

The dark curve in Figure 6 is eustatic sea level (from Haq et al., 1987) averaged over a 10 m.y. running window. Lighter curves in Figure 6 result from different initial rates used for the original ocean basin (equation above). Although there is poor agreement prior to 120 Ma (discussed below), good agreement is seen after this time. Major trends in the eustatic sea-level curve and predicted sea-level height are well matched by using an original ocean basin that is formed from an areal spreading rate of approximately 2×10^6 km^2/m.y. Note the near agreement in the two highest peaks in sea level (at about 90 and 45 Ma), thus accounting for the lag time seen in Figure 5 (it takes an extended period of time for a significant part of older plate to be replaced by younger plate). In view of the large misfit prior to 120 Ma, we may have underestimated spreading rates between 180 and 120 Ma.

For an alternative explanation of the discrepancies seen between 180 and 120 Ma, we return to the discussion involving the dynamic-convection model of Gurnis (1990). In this model, long-term slow spreading rates would allow the sublithospheric mantle to rise in temperature and increase in volume, the result being a rise in sea level for time intervals on the order of 120–240 m.y. after the initiation of slow spreading (Fig. 2 of Gurnis, 1990). If the slower spreading rates seen in our model prior to 130 Ma are approximately correct, and are applicable to earlier times, the misfit in our model prior to 120 Ma is consistent with the dynamic-convection model. Put more optimistically, the pre-120 Ma increase in eustatic sea level suggests that spreading rates were slow for the time period prior to 130 Ma and possibly as far back as about 250 Ma.

Agreement (at least since 120 Ma) between first-order changes in eustatic sea level and predicted changes using simple assumptions about the overall age distribution of lithosphere entering trenches coupled with global spreading rates is encouraging.

SUMMARY

Since 180 Ma, the area of plate (primarily oceanic) now buried in the mantle is approximately equal to the surface area of Earth. Subducted lithosphere is concentrated in regions (lithospheric graveyards), and these regions correspond to gross mantle heterogeneity—the mantle is cold where plate is buried.

More than 13 000 km of convergence has occurred at the Japan Trench and western North America since 150 Ma. Approximately 8000 km has descended beneath the central Andes and the Himalayas, and only about 1000 km of convergence is seen for the western Alps.

With regard to motions of the overriding plates relative to the hotspots (the component orthogonal to their boundaries), North America and South America show a net advance (primarily westward) of about 3000 km. Eurasia, near the Himalayan suture, has advanced approximately 1000 km (southward) with most of this displacement occurring prior to 75 Ma. Although no net orthogonal motion is observed for the Japan Trench, retreat of this trench about 1500 km (eastward) between 150 and 90 Ma was followed by an equivalent advance (westward). Africa, near the western Alps, shows approximately 2200 km of steady trenchward advance (northward). Thus, each of these regions of convergence displays a unique kinematic history. It appears that a significant amount of advance of the overriding plates toward their convergent boundaries is both a necessary and sufficient condition for large-scale crustal uplift and orogeny.

Finally, the pattern of global spreading rates at oceanic ridges is consistent with a first-order eustatic sea-level curve (120 Ma to the present) when a simple model for the age-area distribution within the world's ocean basins is assumed (lithosphere subsidence model). The amount of plate subducted as a function of its age appears directly related to the percentage present. Effects of the dynamic-convection model of Gurnis (1990) may be recorded in the steady rise of eustatic sea level between 180 and 120 Ma and imply a long history of slow spreading prior to 120 Ma.

ACKNOWLEDGMENTS

Supported in part by the Donors of the Petroleum Research Fund, administered by the American Chemical Society, by National Science Foundation grants OCE 8816952 and EAR 8718500, and by a grant from the Institute of Geophysics and Planetary Physics at Los Alamos National Laboratory. We thank E. Moores, T. Tingle, R. Burmester, and an anonymous reviewer for improvement of the manuscript.

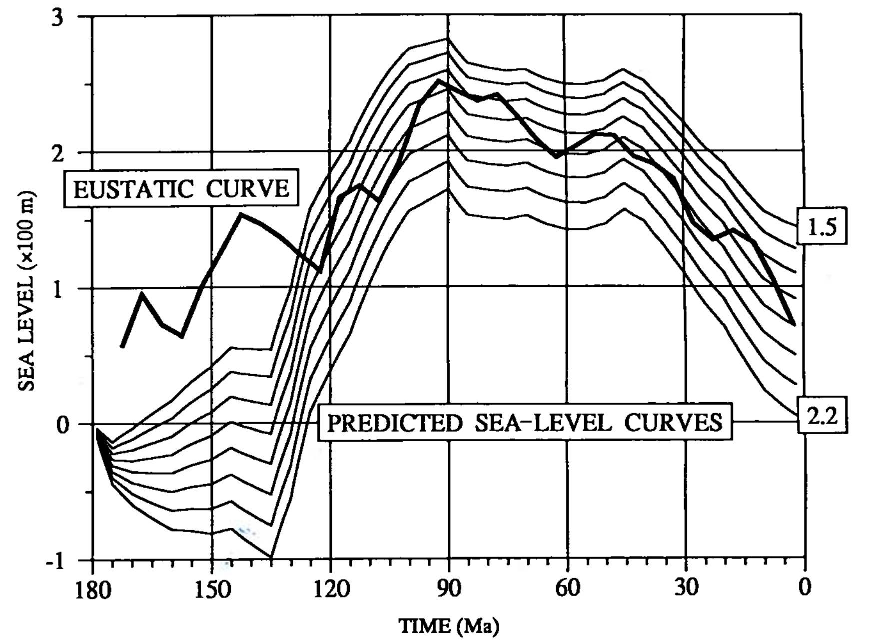

Figure 6. Predicted sea-level curves (light lines) vs. eustatic sea level (heavy curve) of Haq et al. (1987) averaged with a 10 m.y. running window. Numbers on right side of diagram refer to areal rate of spreading (×10^6 km^2/m.y.) used to build the 180 Ma ocean basin.

REFERENCES CITED

Anderson, D.L., 1989, Theory of the Earth: Brookline Village, Maine, Blackwell, 366 p.

Cande, S., LaBrecque, J.L., and Haxby, W.F., 1988, Plate kinematics of the South Atlantic: Chron C34 to present: Journal of Geophysical Research, v. 93, p. 13,479–13,492.

Chase, C.G., 1979, Subduction, the geoid, and lower mantle convection: Nature, v. 282, p. 464–468.

Chase, C.G., and Sprowl, D.R., 1983, The modern geoid and ancient plate boundaries: Earth and Planetary Science Letters, v. 62, p. 314–320.

Davies, G.F., 1984, Lagging mantle convection, the geoid and mantle structure: Earth and Planetary Science Letters, v. 69, p. 187–194.

DeMets, C., Gordon, R.G., Argus, D.F., and Stein, S., 1990, Current plate motions: Geophysical Journal, v. 101, p. 425–478.

Dziewonski, A.M., 1984, Mapping the lower mantle: Determination of lateral heterogeneity in P velocity up to degree and order 6: Journal of Geophysical Research, v. 89, p. 5929–5952.

Engebretson, D.C., Cox, A., and Gordon, R., 1984, Relative motions between oceanic plates of the Pacific basin: Journal of Geophysical Research, v. 89, p. 10,291–10,310.

Engebretson, D.C., Cox, A., and Gordon, R., 1985, Relative motions between oceanic and continental plates in the Pacific basin: Geological Society of America Special Paper 206, 59 p.

Gurnis, M., 1990, Ridge spreading, subduction, and sea level fluctuations: Science, v. 250, p. 970–972.

Hager, B.H., 1980, Eustatic sea level and spreading rate are not simply related: Eos (Transactions, American Geophysical Union), v. 61, p. 374.

Hager, B.H., 1984, Subducted slabs and the geoid: constraints on mantle rheology and flow: Journal of Geophysical Research, v. 89, p. 6003–6015.

Haq, B.U., Hardenbol, J., and Vail, P.R., 1987, Chronology of fluctuating sea levels since the Triassic: Science, v. 235, p. 1136–1165.

Henderson, L.J., Gordon, R.G., and Engebretson, D.C.,1984, Mesozoic aseismic ridges on the Farallon plate and southward migration of shallow subduction during the Laramide orogeny: Tectonics, v. 3, p. 121–132.

Kent, D.V., and Gradstein, F.M., 1986, A Jurassic to recent chronology, *in* Vogt, P.R., and Tucholke, B.E., eds., The western Atlantic region: Boulder, Colorado, Geological Society of America, Geology of North America, v. M, p. 45–50.

Klitgord, K.D., and Schouten, H., 1986, Plate kinematics of the central Atlantic, *in* Vogt, P.R., and Tucholke, B.E., eds., The western Atlantic region: Boulder, Colorado, Geological Society of America, Geology of North America, v. M, p. 351–378.

Kominz, M.A., 1987, Oceanic ridge volumes and sea-level change—An error analysis, *in* Schlee, J.S., ed., Interregional unconformities and hydrocarbon accumulation: American Association of Petroleum Geologists Memoir 36, p. 109–127.

Lerch, F.J., Klosko, S.M., and Patch, G.B., 1983, A refined gravity model from LAGEOS (GEM - L2): NASA Technical Memo TM 84986.

Molnar, P., Pardo-Casas, F., and Stock, J., 1988, The Cenozoic and Late Cretaceous evolution of the Indian Ocean basin: Uncertainties in the reconstructed positions of the Indian, African, and Antarctic plates: Basin Research, v. 1, p. 23–40.

Morgan, W.J., 1983, Hotspot tracks and early rifting of the Atlantic: Tectonophysics, v. 94, p. 123–139.

Nakiboglu, S.M., 1982, Hydrostatic theory of the Earth and its mechanical implications: Physics of the Earth and Planetary Interiors, v. 28, p. 302–311.

Pardo-Casas, F., and Molnar, P., 1987, Relative motion of the Nazca (Farallon) and South American plates since Late Cretaceous time: Tectonics, v. 6, p. 233–248.

Parsons, B., 1982, Cause and consequences between area and age of the ocean floor: Journal of Geophysical Research, v. 87, p. 289–302.

Parsons, B., and Sclater, J.G., 1977, An analysis of the variation of ocean floor bathymetry and heat flow with age: Journal of Geophysical Research, v. 82, p. 803–838.

Pitman, W.C., III, 1978, Relationship between eustacy and stratigraphic sequences of passive margins: Geological Society of America Bulletin, v. 89, p. 1389–1403.

Richards, M.A., and Engebretson, D.C., 1992, The history of subduction, and large-scale mantle convection: Nature, v. 355, p. 437–440.

Richards, M.A., Hager, B.H., and Sleep, N.H., 1988, Dynamically supported geoid highs over hotspots: Observation and theory: Journal of Geophysical Research, v. 93, p. 7690–7708.

Sclater, J.G., Anderson, R.N., and Bell, M.L., 1971, The elevation of ridges and the evolution of the central Pacific: Journal of Geophysical Research, v. 76, p. 7888–7915.

Srivastava, S.P., and Tapscott, C.R., 1986, Plate kinematics of the North Atlantic, *in* Vogt, P.R., and Tucholke, B.E., eds., The North Atlantic region: Boulder, Colorado, Geological Society of America, Geology of North America, v. M, p. 379–404.

Stock, J.M., and Molnar, P., 1988, Uncertainties and implications of the Late Cretaceous and Tertiary position of North America relative to the Farallon, Kula, and Pacific plates: Tectonics, v. 7, p. 1339–1384.

Vail P.R., Mitchum, R.M., Jr., and Thompson, S., III, 1977, Seismic stratigraphy and global changes of sea level, part 4, global cycles of relative changes of sea level, *in* Seismic stratigraphy—Applications to hydrocarbon exploration: American Association of Petroleum Geologists Memoir 26, p. 83–97.

Weissel, J.K., and Hayes, D.E., 1977, Evolution of the Tasman Sea revisited: Earth and Planetary Science Letters, v. 36, p. 77–84.

Wilson, D.S., 1988, Tectonic history of the Juan de Fuca Ridge over the last 40 million years: Journal of Geophysical Research, v. 93, p. 11,863–11,876. ■

Manuscript received January 15, 1992; revision received March 4, 1992; accepted March 6, 1992.